Applied Geochemistry 126 (2021) 104873

Contents lists available at ScienceDirect

Applied Geochemistry

journal homepage: http://www.elsevier.com/locate/apgeochem

Significance of active speleothem $\delta^{18}O$ at annual-decadal timescale——A case study from monitoring in Furong Cave

Hai-Ying Qiu [a,b,1], Ting-Yong Li [c,1,*], Chao-Jun Chen [a], Ran Huang [a], Tao Wang [a], Yao Wu [a], Si-Ya Xiao [a], Yu-Zhen Xu [a], Yang-Yang Huang [a], Jian Zhang [a,d], Yan Yang [a], Jun-Yun Li [a,b,**]

[a] Chongqing Key Laboratory of Karst Environment, School of Geographical Sciences, Southwest University, Chongqing, 400715, China
[b] Key Laboratory of Karst Dynamics, M.N.R. & Guangxi, Institute of Karst Geology, CAGS, Guilin, 541004, China
[c] Yunnan Key Laboratory of Plateau Geographical Processes & Environmental Changes, Faculty of Geography, Yunnan Normal University, Kunming, 650500, China
[d] Environnements et Paléoenvironnements Océaniques et Continentaux (EPOC), UMR CNRS, 5805, Université de Bordeaux, Pessac, France

ARTICLE INFO

Editorial handling by Prof. M. Kersten

Keywords:
Cave monitoring
Active speleothems
$\delta^{18}O$
Isotopic equilibrium fractionation

ABSTRACT

Stalagmites are the product of the combined effects of the surface environment and the cave environment, and their stable carbon and oxygen isotope ratios ($\delta^{18}O$ and $\delta^{13}C$) have been widely used as proxies for palaeoclimatic and palaeoenvironmental reconstructions. Modern cave monitoring is essential for the accurate interpretation of multiple-proxies in stalagmites. However, the interpretation of the climatic and environmental signals indicated by the carbon and oxygen stable isotopes in stalagmites remains controversial. Based on the ongoing monitoring work of Furong Cave in Southwest China over 12 years (2008-2019 AD) involving a combination of field monitoring and experimental data, the following conclusions were drawn. (1) On the interannual scale, the isotopic fractionation of oxygen in active speleothems (AS) exhibits equilibrium fractionation. On the seasonal scale, the crystallization of a mixture of calcite and aragonite minerals is one of the reasons for the deviation of oxygen isotopic composition from the value expected under equilibrium fractionation. (2) There was a significantly positive correlation between $\delta^{18}O$ and $\delta^{13}C$ values in the AS, which may have been controlled by climate change rather than dynamic fractionation. (3) Mainly because of the mixing effect in the 300–500 m of bedrock overlying Furong Cave, the $\delta^{18}O$ value of the drip water reflected the annual average $\delta^{18}O$ value of precipitation. (4) The AS $\delta^{18}O$ ($\delta^{18}O_{AS}$) values over the 12-year monitoring records did not show significant seasonal variations but exhibited multiyear trend, which might reflect changes in the external atmospheric circulation and "amount effect" on decadal and longer timescales. Consequently, speleothem $\delta^{18}O$ values in Furong Cave can be used for isotope-based palaeoclimate reconstruction.

1. Introduction

Stalagmites have become an important archive of palaeoclimate research because of their high-precision dating and high-resolution multiproxy records (Fleitmann et al., 2004; Yuan et al., 2004; Li et al., 2011a; Cheng et al., 2012). Stable isotopes (oxygen and carbon) are the most widely used proxies in stalagmites (Wang et al., 2001; Zeng et al., 2015). The carbon and oxygen stable isotopes of stalagmites deposited in the state of isotopic equilibrium fractionation can record palaeoenvironmental information (Hendy, 1971). However, the cave temperature, CO_2 degassing, drip rate and the relative humidity of the air may cause nonequilibrium fractionation (Mickler et al., 2006; Fairchild et al., 2006; Coplen, 2007; Dietzel et al., 2009; Day and Henderson, 2011; Feng et al., 2014), which may alter the climate signal, resulting in an inaccurate interpretation of the proxies in geologic archives. Speleothem $\delta^{18}O$ values are commonly related to the $\delta^{18}O$ values of cave drip water derived from surface rainfall. To date, the indicative significance of precipitation $\delta^{18}O$ values is still contested. For example, precipitation $\delta^{18}O$ values may be dominated by the temperature effect, amount effect, circulation effect, rainout effect and convective activity

* Corresponding author. Yunnan Key Laboratory of Plateau Geographical Processes & Environmental Changes, Faculty of Geography, Yunnan Normal University, Kunming, 650500, China.
** Corresponding author. Chongqing Key Laboratory of Karst Environment, School of Geographical Sciences, Southwest University, Chongqing, 400715, China.
E-mail addresses: cdlity@163.com (T.-Y. Li), jxljy@swu.edu.cn (J.-Y. Li).
[1] Joint first authors: Hai-Ying Qiu and Ting-Yong Li.

https://doi.org/10.1016/j.apgeochem.2021.104873
Received 12 August 2020; Received in revised form 4 January 2021; Accepted 5 January 2021
Available online 8 January 2021

over primary moisture source regions (Fleitmann et al., 2004; Lee et al., 2007; Liu et al., 2008; Dayem et al., 2010; Tan, 2014; Moore et al., 2014; Ruan et al., 2019).

In addition, the covariance of carbon and oxygen isotopes in stalagmites is not necessarily caused by dynamic fractionation (Fairchild et al., 2006; Dorale and Liu, 2009; Zhang et al., 2013). Changes in the ecological environment, biological processes, and hydrological conditions indicated by stalagmite $\delta^{13}C$ values can be robustly related to the climate changes indicated by $\delta^{18}O$ values (Holmgren et al., 1995; Hodge et al., 2008; Scholz et al., 2012; Li and Li, 2018; Li et al., 2018). Speleothem $\delta^{18}O$ and $\delta^{13}C$ values are covariant on the centennial timescale, which has been confirmed by many stalagmite records in China (Cosford et al., 2009; Kuo et al., 2011; Liu et al., 2016; Wu et al., 2020). Consequently, continuous cave monitoring has been recognized as an essential method for clarifying the climatic and environmental significance of proxies in stalagmites (Johnson, 2006; Baldini et al., 2008; Tan, 2014; Li et al., 2017, 2018; Chen and Li, 2018).

The ongoing monitoring research in Furong Cave in Southwest China has been carried out since 2005 AD. The geochemical characteristics and influencing factors of local precipitation, soil water, and cave drip water, have been systematically studied (Li et al., 2011b, 2012, 2018; Li and Li, 2018; Zhang and Li, 2019). Due to the mixing effect in the 300–500 m thick bedrock above Furong Cave, the monitoring data collected over 1–2 years failed to record a pattern similar to the seasonal cycle in the $\delta^{18}O$ values of local precipitation (Li et al., 2011b). In addition, it is also impossible to conduct a detailed comparison between the precipitation and drip water on a monthly timescale (Zhang and Li, 2019). Previous monitoring work in Furong Cave only focused on atmospheric precipitation, soil water, and drip water, and few studies have focused on active speleothems (AS) (Li et al., 2011b, 2018; Li and Li, 2018; Li, 2018; Zhang and Li, 2019). Furthermore, on the interannual to decade timescale, it is still unknown whether AS in Furong Cave record the long-term variation trend in precipitation $\delta^{18}O$ values.

The contributions of the study can be summarized follows: (1) We evaluate the equilibrium fractionation situation of $\delta^{18}O_{AS}$ values. (2) The long-term variation in $\delta^{18}O_{AS}$ values and its climatic and environmental significance are discussed. This study has essential scientific relevance for the reconstruction of palaeoclimate based on speleothem $\delta^{18}O$ data in the East Asian monsoon (EAM) region.

2. Study area and monitoring sites

Furong Cave (29°13′44″ N, 107°54′13″ E) is located in the Cambrian limestone and dolomite strata of the eastern bank of the Furong River, which is a secondary branch of the Yangtze River, Chongqing, southwestern China (Fig. 1A and B). The overlying bedrock is 300–500 m thick, the elevation at the cave entrance is 480 m above sea level (a.s.l.), the cave air temperature is 16.3 °C, and the humidity is 95–100% (Li et al., 2011b; Li and Li, 2018). Furthermore, the regional climate is dominated by the Asian monsoon system and is characterized by cold, dry winters and hot, wet summers. The current annual average precipitation is 1200 mm, with 70% of the annual rainfall occurring during the wet season from May to October (Li et al., 2011b).

Five drip water monitoring sites (MP1, MP2, MP3, MP4, and MP5) were chosen in a tunnel far from the entrance of Furong Cave (Fig. 1C). The drip height of MP1 was approximately 22 m, and each water droplet split into multiple droplets during the process of falling. MP2 was located on the top of a 2 m-high stalagmite, with a falling height of 27 m. MP3 was on the cavity wall, with a short soda-straw stalactite as the outlet, and the drip height was 0.3 m (Li et al., 2011b; Zhang and Li, 2019). The distance between MP4 and MP5 was 1.5 m, and the drip heights were 14 m and 13 m, respectively (Zhang and Li, 2019).

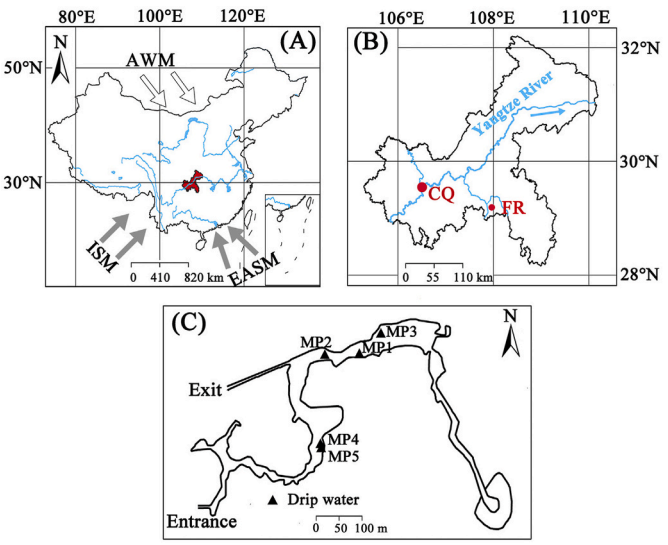

Fig. 1. The geographical location of the study area. (A) Furong Cave is located in Southwest China. The grey arrows indicate the Indian summer monsoon (ISM) and the East Asian summer monsoon (EASM), and the white arrows indicate the Asian winter monsoon (AWM). (B) Red dots indicate the location of Furong Cave (FR) and Chongqing city (CQ). (C) Sketch of Furong Cave and distribution of monitoring sites (black triangle, MP1-MP5), modified after (Li et al., 2011b). (For interpretation of the references to colour in this figure legend, the reader is referred to the Web version of this article.)

3. Data and methods

3.1. Meteorological data and back trajectory model

The air temperature was continuously recorded at 2-h intervals by a temperature recorder (U12-011, Onset, USA), with a measurement range of −40–70 °C, and an error of ±0.1 °C. Precipitation was recorded using an automatic rainfall monitoring instrument (RG3-M, Onset, USA.) at a frequency of once every 2 min, with the precision being ±1.0%. The rainfall monitoring instrument was installed at a height of 1.5 m above the floor, approximately 100 m from the cave entrance. The HYSPLIT (Hybrid Single-Particle Lagrangian Integrated Trajectory Model) (Challa et al., 2008; Stein et al., 2015; Cai et al., 2018; Zhang et al., 2020), NCEP (National Centers for Environmental Prediction), and NOAA (National Oceanic and Atmospheric Administration) reanalysis data sets (ftp://arlftp.arlhp.noaa.gov/pub/archives/reanalysis) were used to simulate air mass trajectories to determine the moisture sources in summer (June to August) from 2008 to 2019 AD and to cluster the moisture trajectories (Table 1). Trajectory analysis was performed

Table 1
Proportion of moisture sources and the weighted $\delta^{18}O$ of summer precipitation in Chongqing from 2008 to 2019 (A.D).

Year (A.D)	Indian Ocean (%)	Pacific Ocean (%)	Other sources (%)	Amount weighted $\delta^{18}O$ (V-SMOW, ‰) (June–August)
2008	53	21	26	−8.50
2009	59	36	5	−9.40
2010	58	14	28	−8.60
2011	45	12	43	−8.11
2012	56	11	33	−9.72
2013	50	33	17	−8.60
2014	47	45	8	−8.31
2015	38	37	25	−7.16
2016	58	35	7	−8.31
2017	47	11	42	−7.97
2018	46	19	35	−8.70
2019	32	22	46	−7.94

four times every day (at UTC 00:00, 06:00, 12:00, and 18:00); the simulation height was set at 850 hPa, and the air masses were moved backwards for 240 h (10 days) (Sun et al., 2018).

3.2. Water samples collection and measurement

A rainwater collection device — a plastic bucket with a funnel — was set outside Furong Cave. The specific steps and methods were described by Zhou and Li (2018). A polyethene bottle for collecting drip water, 30 ml in volume, was soaked in a 5% nitric acid solution for 5 h, rinsed with ultrapure water and naturally dried in an ultrapure room. The prepared polyethene bottles were placed under each drip site to collect drip water and were subsequently sealed in the cave and put into a laboratory refrigerator (5 °C) within 24 h for the isotope test. Water samples (with a volume of 1.5 ml) were analysed by a liquid isotope analyser (LWIADLT-100, Los Gatos) for the analysis of the δ^2H and $\delta^{18}O$ values of the water. Each sample was analysed six times, and the average value of the last four measurements was used as the final value. LGR3A, LGR4A, and LGR5A (Los Gatos Research, USA.) were used as reference standards, and all results were reported in per mil (‰) relative to the Vienna Standard Mean Ocean Water (V-SMOW) standard. The absolute errors of the $\delta^{18}O$ and δ^2H measurements were less than 0.2‰ and 0.5‰, respectively (Zhang and Li, 2019).

3.3. Active speleothem collection and measurement

Clean glass plates with a diameter of 10 cm and a thickness of 1 mm were placed under five drip sites (MP1-MP5) to collect AS material. These plates were collected every three months (due to the breakage or loss of some glass plates, the samples in some periods are missing), and dried at 60 °C in the laboratory. A clean knife was used to scrape 20–50 μg of AS powder from the glass plates. The measurements were performed using an isotope ratio mass spectrometer, specifically, a Finnegan DELTA V PLUS coupled with a Kiel IV automated carbonate device at the Laboratory of Geochemistry and Isotopes, Southwest University, China. Measurements of an international standard, NBS19, and an inhouse standard, SWU1, show a one-sigma reproducibility of ±0.10‰ for $\delta^{18}O$ and ±0.06‰ for $\delta^{13}C$. The detailed analysis methods were described by Li et al. (2011b). All AS isotope data are reported in per mil (‰) relative to the Vienna Pee Dee Belemnite (V-PDB) standard. A polarizing microscope (ECLIPSE Nikon E600W POL) was used to observe the morphological composition of the five glass plates of speleothems during the monitoring period.

4. Results

4.1. Precipitation $\delta^{18}O$

The range of precipitation $\delta^{18}O$ values during the monitoring period was −14.28‰ ~ −0.54‰, the monthly amount-weighted $\delta^{18}O$ value of precipitation was −7.58‰, and the standard deviation (1σ) was 3.18‰ (Table 2). On the interannual timescale, the $\delta^{18}O$ values of precipitation from 2008 to 2019 AD and the amount-weighted $\delta^{18}O$ values of precipitation in the rainy season (April–October) exhibited an overall positive trend (Fig. 2A and B).

4.2. Drip water $\delta^{18}O$

The ranges of $\delta^{18}O$ values in the MP1-MP5 drip water were −5.21‰ ~ −8.14‰, −4.80‰ ~ −8.39‰, −6.26‰ ~ −7.96‰, −5.89‰ ~ −8.37‰, and −6.03‰ ~ −8.79‰, respectively (Fig. 3, Table 2). The multiyear averages of drip water $\delta^{18}O$ values were −7.04 ± 0.73‰, −7.19 ± 0.76‰, −7.29 ± 0.70‰, −7.43 ± 0.36‰, and −7.51 ± 0.34‰ (Table 2). There was no clear seasonal change in the $\delta^{18}O$ values of drip water during the entire monitoring period (Fig. 3A–E). However, the $\delta^{18}O$ of drip water was significantly higher from December 2014 to February 2015, and significantly lower in summer 2017 (Fig. 3A–E). These two anomalies may be attributed to the potential response of the drip water $\delta^{18}O$ values to El Niño-Southern Oscillation (ENSO) (Zhang and Li, 2019). In addition, except for MP1, the variations in drip water $\delta^{18}O$ values at the other four sites were generally consistent in 2011-2019 AD, showing a positive trend before 2015 AD and a weak negative/positive trend before/after the minimum $\delta^{18}O$ values in the summer of 2017 AD (Fig. 3A–E).

Table 2
$\delta^{18}O$ values of precipitation, drip water, and active speleothems.

Sample		Minimum	Mean	Maximum	±1σ	Sample number (n)
Precipitation $\delta^{18}O$ (V-SMOW, ‰)		−14.28	−7.58	0.54	3.18	130
Drip water $\delta^{18}O$ (V-SMOW, ‰)	MP1	−8.14	−7.04	−5.12	0.73	132
	MP2	−8.39	−7.19	−4.80	0.76	132
	MP3	−7.96	−7.29	−6.26	0.70	123
	MP4	−8.37	−7.43	−5.89	0.36	122
	MP5	−8.79	−7.51	−6.03	0.34	123
Active speleothems $\delta^{18}O$ (V-PDB, ‰)	MP1	−7.36	−6.91	−6.52	0.23	41
	MP2	−7.38	−7.01	−6.63	0.17	41
	MP3	−7.38	−7.12	−6.77	0.14	39
	MP4	−7.78	−7.40	−6.42	0.39	42
	MP5	−7.73	−7.49	−6.56	0.28	42

4.3. Active speleothem $\delta^{18}O$ values and morphological composition

The AS $\delta^{18}O$ values of MP1-MP5 ranged from −6.52‰ ~ −7.36‰, −6.63‰ ~ −7.38‰, −6.77‰ ~ −7.38‰, −6.42‰ ~ −7.78‰, and −6.56‰ ~ −7.73‰, respectively (Fig. 4A–E, Table 2). The average AS $\delta^{18}O$ values of MP1-MP5 were −6.91 ± 0.23‰, −7.01 ± 0.17‰, −7.12 ± 0.14‰, −7.40 ± 0.39‰, and −7.49 ± 0.28‰ (Table 2). Unlike the $\delta^{18}O$ values of drip water, the $\delta^{18}O$ values of the AS at the five drip sites appeared to show a weak seasonal cycle during the monitoring period, with lower values in summer and higher values in winter, with the largest amplitude of the seasonal variation being less than 0.5‰ (Fig. 4). However, taking drip site MP1 as an example, this seasonal characteristic of AS $\delta^{18}O$ values is contrary to the seasonal variation in the drip water $\delta^{18}O$ values (Figs. 3A and 4A). In addition, in 2019 AD, the $\delta^{18}O$ values of the AS were higher in summer and lower in winter at all drip sites, opposite the seasonal variation observed in other years (Fig. 4). Except for the anomaly in 2019 AD, the variation in AS $\delta^{18}O$ values generally showed a negative trend, followed by a positive trend, although the timing of the transition was different at each site (Fig. 4A–E). Polarization microscopy observation results showed that MP1, MP4, and MP5 are mixtures of rhombi and acicula (Fig. 5A, D, 5E), while MP2 and MP3 are purely calcite rhombi (Fig. 5B and C).

4.4. Changes in moisture source

The HYSPLIT model was used to calculate the change in the moisture contribution ratio in summer (June–August) during the period of 2008-2019 AD in Chongqing (Table 1). The Indian Ocean (IO) is the principal moisture source for precipitation in the Asian summer monsoon. The moisture from the IO accounts for 38%–59% (with an average of 49%) of all vapor. On the other hand, the proportions of moisture from the Pacific Ocean and other sources (westerlies and the continent) amount to 11% ~ 45% (with an average of 25%) and 5% ~ 46% (with an average of 26%), respectively (Table 1). During the summer months in this monitoring period, the moisture originating from the IO presented a decreasing trend, while moisture from other sources outside the IO (e.g., from the Pacific Ocean, the South China Sea, westerlies, or the continent) showed an increasing trend (Fig. 2C).

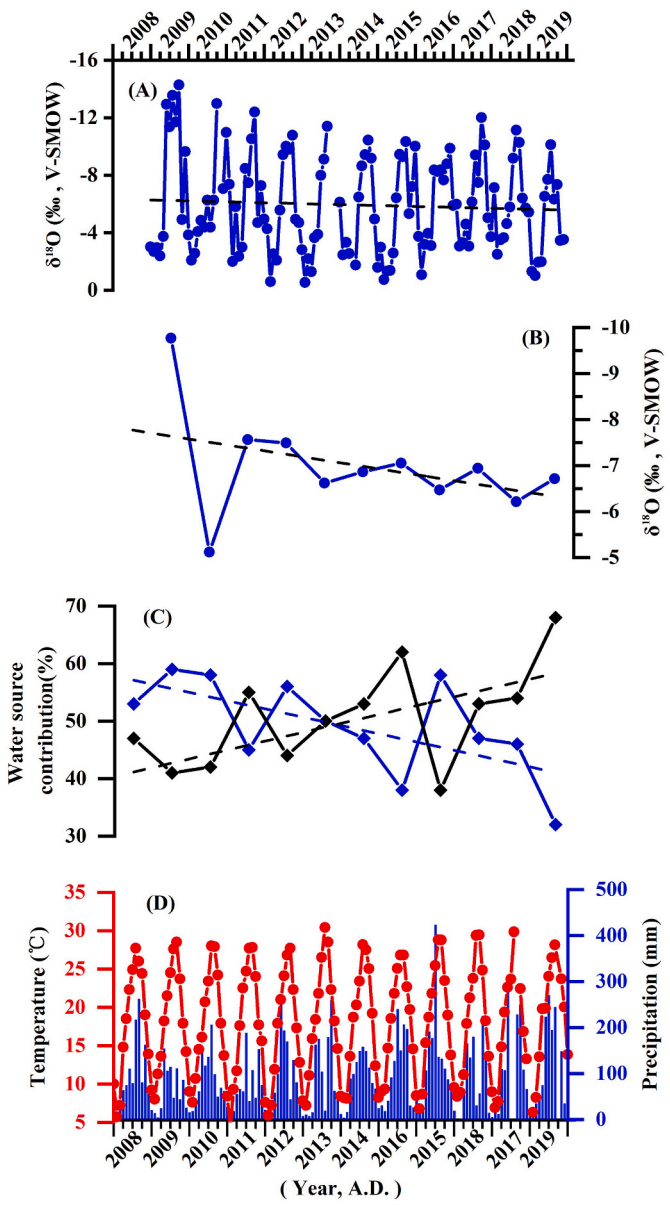

Fig. 2. (A) Original data of monthly precipitation $\delta^{18}O$; (B) Amount weighted $\delta^{18}O$ of precipitation from April to October; (C) Proportion of moisture source in summer (June–August) based on the analyses of the HYSPLIT model. The blue curve indicates the proportion of moisture from the Indian Ocean, and the black curve represents the proportion of moisture from other sources (the Pacific Ocean and the South China Sea, as well as westerlies and the continent); (D) Monthly precipitation and average air temperature outside Furong Cave. All dotted lines in the panels are linear trend lines based on the least squares method. (For interpretation of the references to colour in this figure legend, the reader is referred to the Web version of this article.)

5. Discussion

5.1. Testing equilibrium fractionation for oxygen isotope

Speleothems deposited under isotopic equilibrium fractionation can inherit the stable oxygen and carbon isotopic compositions of the drip water (Faichild et al., 2006). The equilibrium fractionation of $^{18}O/^{16}O$ in aragonite and calcite controlled by the drip water $\delta^{18}O$ value and the cave temperature (Kluge et al., 2014; Lachniet, 2015). The equations for the deposition of aragonite (Equation (1); Kim et al., 2007) and calcite (Equation (2); Tremaine et al., 2011) were used to calculate the theoretical $\delta^{18}O$ values under equilibrium fractionation. Equation (3) was used to convert drip water $\delta^{18}O$ values from the V-SMOW standard to the V-PDB standard (Coplen et al., 1983). The theoretical AS $\delta^{18}O$ values calculated by the above three equations were compared with the actual AS $\delta^{18}O$ values obtained from the material deposited on the glass plates (Table 3). If the difference between the theoretical values and the actual values is less than 0.2‰, the speleothems can be considered to have been deposited under isotopic equilibrium fractionation (Mickler et al., 2004).

$$1000 \ln \alpha = 17.88 \times 1000/T - 31.14 \quad (1)$$

$$1000 \ln \alpha = 16.01 \times 1000/T - 24.60 \quad (2)$$

$$\delta^{18}O_{V-PDB} = 0.97002 \times \delta^{18}O_{V-SMOW} - 29.98 \quad (3)$$

$$\alpha = \left(\delta^{18}O_{carbonate} + 1000\right)/\left(\delta^{18}O_{water} + 1000\right) \quad (4)$$

α represents the $^{18}O/^{16}O$ fractionation coefficient of carbonate deposits, and T is the absolute temperature (Kelvin). It should be noted that the AS at MP1, MP4, and MP5 were composed of aragonite and calcite minerals (Fig. 4). Aragonite and calcite cannot be manually separated when sampling the deposits on the glass plates for the analysis of stable isotopic compositions. We calculated the theoretical values of the deposits under equilibrium fractionation by using the aragonite and calcite equations. For all five monitoring sites, on the interannual timescale, the differences between the average AS $\delta^{18}O$ values at MP1-MP5 and the theoretical average $\delta^{18}O$ values are 0.07‰–0.12‰, 0.09‰, 0.03‰, 0.02‰–0.08‰, and 0.03‰–0.14‰ (Table 3). The mixed deposition of calcite and aragonite minerals (MP1, MP4, and MP5) (Fig. 5A, D, and 5E) may be the main reason for the slight deviation between the theoretical and actual values. The comparisons between the calculated values and the analysed values indicate that the deposition of AS in Furong Cave occurs under isotopic equilibrium fractionation.

5.2. Positive correlations between $\delta^{18}O_{AS}$ and $\delta^{13}C_{AS}$

At all the drip sites, there are significant correlations between the $\delta^{18}O$ and $\delta^{13}C$ values of the AS (Fig. 6). Previous studies have attributed the significant correlation between the $\delta^{18}O$ and $\delta^{13}C$ values of calcium carbonate to dynamic fractionation (Hendy, 1971; Laskar et al., 2011). However, the covariant changes in stalagmite $\delta^{18}O$ and $\delta^{13}C$ values at the centennial to millennial timescales, even at the orbital timescale, have been confirmed by many geologic records, indicating that the changes in $\delta^{18}O$ and $\delta^{13}C$ values are controlled by the same climate-driven mechanism (Li et al., 2012, 2018; Liu et al., 2016; Wu et al., 2020). Many factors influence the carbon isotopic composition of soil water, including the type and density of local plants, the activity of microbes, and the concentration of CO_2 in soil, which is dominantly controlled by the temperature and humidity of the soil (Bar-Matthews et al., 1996; Li et al., 2018). Surface vegetation is heavily affected by the local climate and environment, especially the surface hydrological conditions.

Long-term monitoring results confirmed that the change in the $\delta^{13}C$ values of dissolved inorganic carbon ($\delta^{13}C_{DIC}$) in drip water in Furong Cave occurred in response to changes in local precipitation on a decadal timescale, with negative $\delta^{13}C_{DIC}$ values corresponding to more precipitation (Li and Li, 2018). It is well known that the $\delta^{13}C$ value of drip water is not only controlled by surface vegetation and soil CO_2 but is also affected by the $\delta^{13}C$ composition of the bedrock (Bar-Matthews et al., 1996; Baker et al., 1997; Linge, 2001). Both surface biological processes and physicochemical processes (e.g. water-rock interaction) during the migration of karst groundwater are regulated by local hydrological conditions (Sondag et al., 2003; Treble et al., 2005; Baker et al., 2007; Li et al., 2018). Therefore, we propose that the significant positive correlation between the $\delta^{18}O$ and $\delta^{13}C$ values of AS in Furong Cave was mainly controlled by regional climate change and local hydrological conditions rather than by dynamic fractionation.

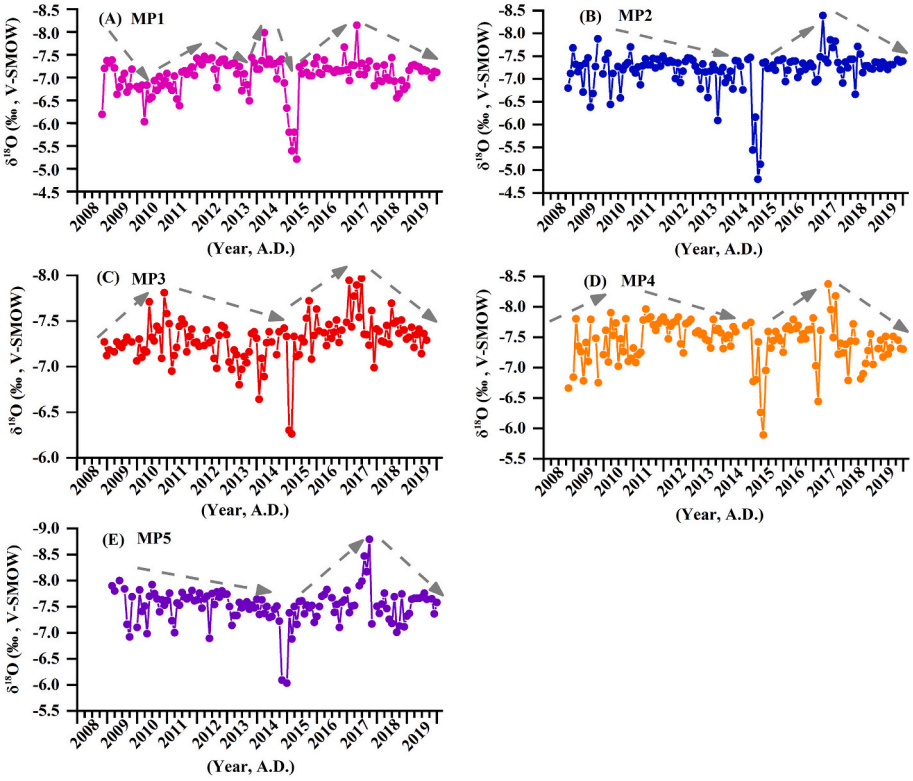

Fig. 3. Variation in the $\delta^{18}O$ values of drip water at five sites during the period of 2008-2019 AD. The grey dashed arrows indicate the stage characteristics.

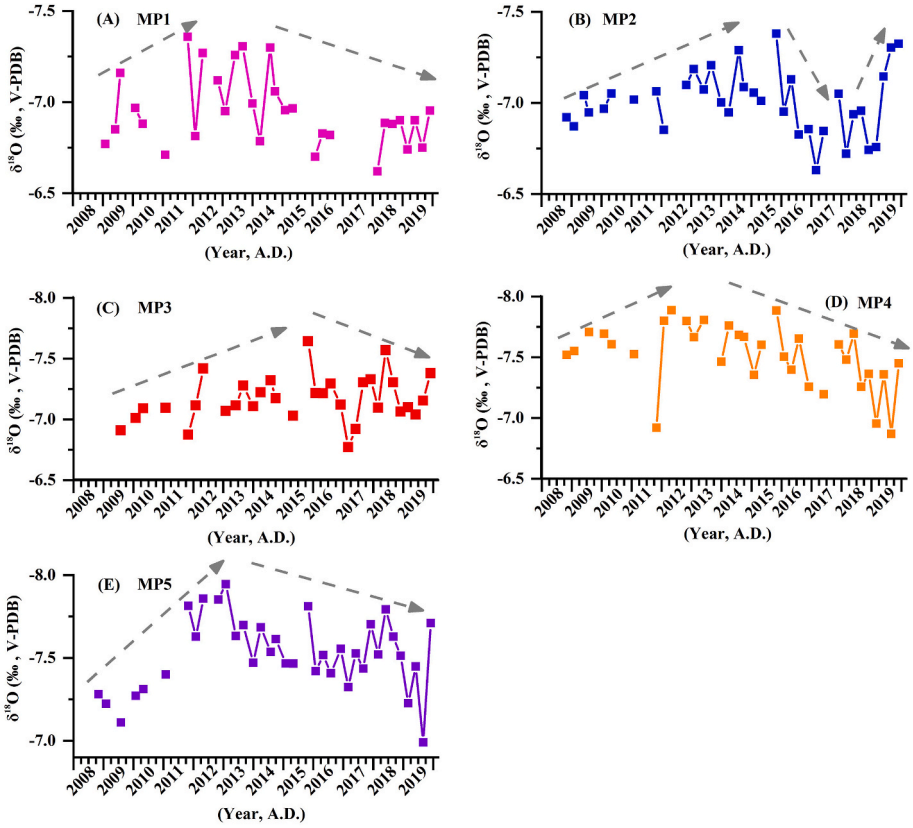

Fig. 4. Variation in the $\delta^{18}O$ values of AS at five sites from 2008-2019 AD. The grey dashed arrows indicate general trend in different stages.

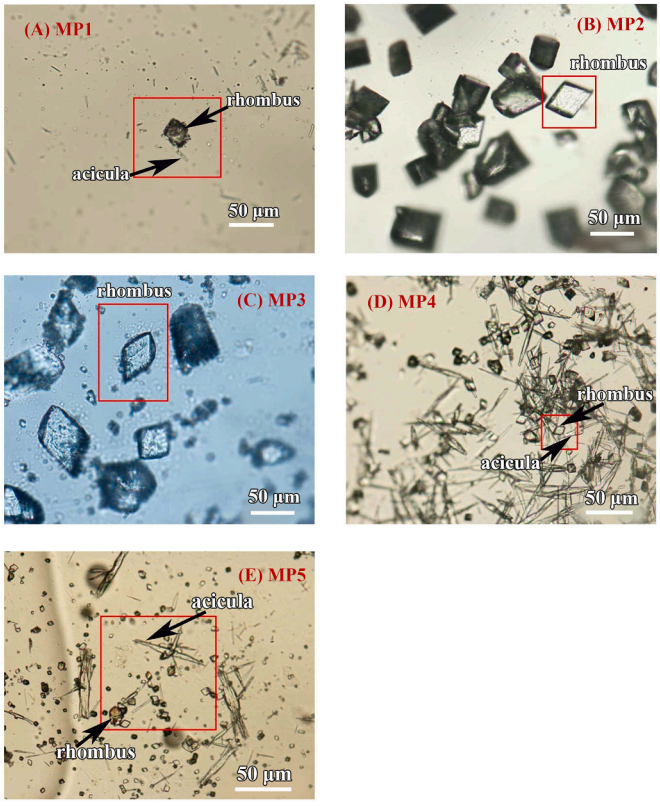

Fig. 5. Morphological compositions of AS deposited on glass plates at the monitoring drip sites. (A) MP1, (B) MP2, (C) MP3, (D) MP4, (E) MP5. The mineral compositions of the deposits at MP1, MP4, and MP5 are mixtures of rhombi and acicula, while those at MP2 and MP3 are purely calcite rhombi.

5.3. Precipitation $\delta^{18}O$ responding to changes in moisture sources

During the monitoring period from 2008 to 2019 AD, there was no significant negative correlation between precipitation and precipitation $\delta^{18}O$ values in summer (June to August) ($r = 0.12$, $p < 0.01$). However, there was a negative correlation between original monthly precipitation and $\delta^{18}O$ value on the annual timescale ($r = -0.33$, $p < 0.01$). Similar to the interannual scale, there was a negative correlation between original monthly precipitation and $\delta^{18}O$ value from April to June in 2008-2019AD ($r = -0.12$, $p < 0.01$). The results indicate that the "amount effect" does exist in the study area and the influence factors of the local $\delta^{18}O_p$ are various, it can be affected by rainfall amount, fractionation temperature and moisture source.

The period from mid-late May to early June is well known for the onset of the Indian summer monsoon (ISM) and arrival of the East Asian rainy season (Li and Qu, 2000; Jin and Tao, 2002; Ding et al., 2014; Cheng et al., 2005; Lü et al., 2006; Chow et al., 2008). The water vapor in summer months mainly comes from the IO, South China Sea (SCS) and West Pacific Ocean (WPO), and the arrival of this water vapor is associated with abundant precipitation. In sharp contrast, during the winter and early spring seasons, the water vapor mainly originates from the evaporation of inland water or short-distance sources, such as the SCS, resulting in positive precipitation $\delta^{18}O$ values.

Previous studies have shown that precipitation and the $\delta^{18}O$ values in monsoon China may be mainly regulated by the circulation effect or the rainout effect (Tan, 2009, 2014; Li, 2018). The IO is the primary moisture source of summer precipitation in the EAM region (Hu et al., 2008; Xie et al., 2011; Liu et al., 2015; Yang et al., 2016; Ding et al., 2014). Compared with the moisture from the SCS and the WPO, the moisture from the IO travels a relatively long distance (Tan, 2014). During the transport of water vapor from moisture sources to inland, the heavy isotopes (^2H and ^{18}O) preferentially condense during the formation of precipitation, resulting in a depleted isotopic composition in the residual water vapor (Ishizaki et al., 2012; Cai and Tian, 2016; Ruan et al., 2019). In summer months, along with the increase of distance from the oceanic moisture source, this so-called "rainout effect" leads to lower precipitation $\delta^{18}O$ values in Chongqing and monsoon China, which are located in a downstream EAM region (Nan et al., 2014; Tan, 2014, 2016; Tang et al., 2015; Yang et al., 2016; Li, 2018). However, moisture from the WPO and the SCS is transported a relatively short distance to the EAM regions, and this relatively short migration distance leads to precipitation with higher $\delta^{18}O$ values than the precipitation originating from IO-derived vapor (Tan, 2014; Liu et al., 2015). Additional moisture comes from the continental interior and the westerlies. Due to secondary evaporation under clouds and local moisture supplementation, the $\delta^{18}O$ values of this fraction of moisture are relatively high (Tang et al., 2015). Therefore, the decreasing proportion of long-distance moisture and the increasing proportion of other moisture on the interannual scale may be an important reason for the apparent positive trend in precipitation $\delta^{18}O$ values outside Furong Cave (Fig. 2A, B, and 2C).

5.4. $\delta^{18}O$ of drip water and speleothems respond to precipitation $\delta^{18}O$

Previous studies have shown that the mixing of precipitation in bedrock above caves can smooth the seasonal changes in isotopic composition in precipitation (Li et al., 2011b; Duan et al., 2016). The response of drip water $\delta^{18}O$ values and speleothem $\delta^{18}O$ values to precipitation $\delta^{18}O$ values is heavily influenced by thick overlying bedrock (Caballero et al., 1996; Perrin et al., 2003; McDonald and Drysdale, 2007; Breitenbach et al., 2015). In addition, mixing of old and young water masses, evaporation in the soil and epikarst zone, and fracture development may modify the original precipitation $\delta^{18}O$ values (Mühlinghaus et al., 2009; Pape et al., 2010; Wackerbarth et al., 2010; Genty et al., 2014; Moerman et al., 2014; Comas-Bru et al., 2015). In this study, compared with the general smooth change in $\delta^{18}O$ during the entire monitoring period, abnormal changes in drip water $\delta^{18}O$ occurred in the winter period between 2014 and 2015 AD and in the summer period of 2017 AD and may have been influenced by changes in moisture source, which potentially occurred in response to changes in atmospheric

Table 3
Comparison between actual $\delta^{18}O$ of active speleothems and theoretical $\delta^{18}O$ for carbonate deposited at isotopic equilibrium fractionation.

Site	$\delta^{18}O_W$ (V-SMOW, ‰)		T_w(°C)	$\delta^{18}O_C$ (V-PDB, ‰)		$\delta^{18}O_E$ (V-PDB, ‰)		$\triangle^{18}O_{C\text{-}E}$ (V-PDB, ‰)
	Mean	±1σ		Mean	±1σ	Equation (1)	Equation (2)	
MP1	−7.07	±0.28	16.38	−6.91	±0.23	−7.03	−6.98	0.07–0.12
MP2	−7.13	±0.14	16.47	−7.01	±0.17	Pure calcite	−7.10	0.09
MP3	−7.28	±0.17	16.41	−7.12	±0.14	Pure calcite	−7.15	0.03
MP4	−7.43	±0.25	17.46	−7.40	±0.39	−7.48	−7.38	0.02–0.08
MP5	−7.32	±0.24	17.71	−7.49	±0.26	−7.63	−7.52	0.03–0.14

The $\delta^{18}O_w$ and T_w represent the drip water $\delta^{18}O$ and the deposition temperature, respectively. $\delta^{18}O_C$ is the actual $\delta^{18}O$ for active speleothems (aragonite or calcite); $\delta^{18}O_E$ is the theoretical $\delta^{18}O$ at isotopic equilibrium fractionation calculated by Equations (1) and (2) (in Section 5.1); and $\triangle^{18}O_{C\text{-}E}$ is the difference between actual $\delta^{18}O$ and theoretical $\delta^{18}O$, which have been used to assess the extent of isotopic fractionation.

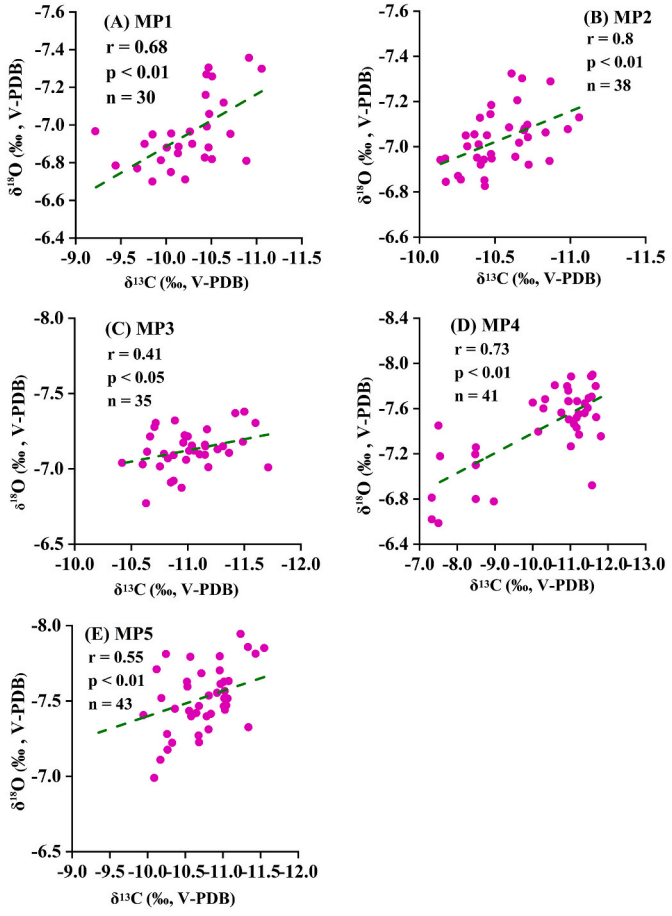

Fig. 6. Correlation between the $\delta^{18}O$ and $\delta^{13}C$ values of AS at the MP1-MP5 monitoring sites. Green dotted lines in the panels are linear trend lines based on the least squares method. (For interpretation of the references to colour in this figure legend, the reader is referred to the Web version of this article.)

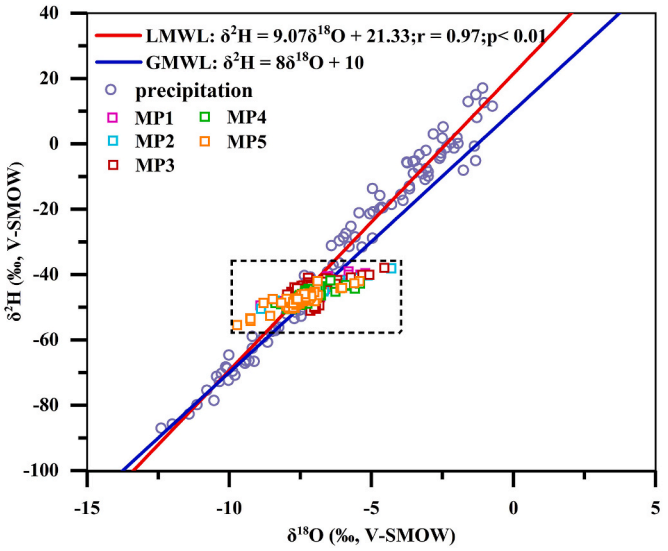

Fig. 7. Comparison between the global meteoric water line (GMWL) (blue line) and the local meteoric water line (LMWL) (red line), which is based on the $\delta^{18}O$ and $\delta^{2}H$ values of precipitation outside Furong Cave (light purple circles). Because of the mixing effect in the hundreds of metres of bedrock overlying the cave, the distribution ranges of the $\delta^{18}O$ and $\delta^{2}H$ values of drip water are obviously smaller than those of precipitation. (For interpretation of the references to colour in this figure legend, the reader is referred to the Web version of this article.)

circulation patterns, such as El Niño and La Niña scenarios (Chen and Li, 2018; Zhou and Li, 2018; Zhang and Li, 2019). The different seasonal variation in the $\delta^{18}O$ values between AS and drip water may result from changes in the cave environment, such as CO_2 degassing, cave temperature, humidity, ventilation, and drip rate (Spötl et al., 2005; Wiedner et al., 2008; Riechelmann et al., 2013). Furthermore, the magnitudes of the $\delta^{18}O$ variations in drip water and AS are smaller than that of the $\delta^{18}O$ variations in precipitation (Li et al., 2011b; Zhang and Li, 2019). The distributions of drip water $\delta^{2}H$ and $\delta^{18}O$ values were concentrated near the local meteoric water line (LMWL) (Fig. 7), indicating that the $\delta^{2}H$ and $\delta^{18}O$ values of drip water represented averages of the precipitation isotopic composition on the multiyear timescale. In the well-enclosed Furong Cave, the deposition of AS occurs under isotopic equilibrium fractionation. There is no doubt that the $\delta^{18}O$ value of AS in Furong cave is a lagging and mixed expression of the precipitation $\delta^{18}O$ value. A high-resolution (e.g., seasonal and annual) $\delta^{18}O$ record of AS in Furong Cave may be unavailable. However, the $\delta^{18}O$ records of speleothems in Furong Cave maybe reflect the long-term trend of local precipitation $\delta^{18}O$ values on decadal and longer timescales. Therefore, the stalagmites in Furong Cave can be used in the reconstruction of palaeoclimate and paleoenvironment changes on decadal and longer timescales (Li and Li, 2018; Zhang and Li, 2019).

6. Conclusions

Based on the continuous monitoring of drip water and AS in Furong Cave overlain by 300–500 m of bedrock, the climatic and environmental significance of AS $\delta^{18}O$ values has been investigated. The deposition of AS occurred under isotopic equilibrium fractionation on an interannual timescale. The mixed deposition of calcite and aragonite minerals may be part of the reason for the deviation between the actual $\delta^{18}O$ values and the calculated $\delta^{18}O$ values under isotopic equilibrium fractionation. There was a significant positive correlation between the $\delta^{18}O$ and $\delta^{13}C$ values of AS, which was mainly controlled by the changes in the climate and regional hydrological conditions rather than by dynamic fractionation. As a major influencing factor, the mixing effect in the hundreds of metres of bedrock overlying the cave resulted in relatively stable $\delta^{18}O$ values in the drip water and AS, without an obvious seasonal cycle. Due to the mixing and lag transportation in the 300–500m vadose zone, the high-resolution (e.g., seasonal and annual) $\delta^{18}O$ record in AS in Furong Cave, which is overlain by hundreds of metres of bedrock, may be unavailable. For a stalagmite record longer than 100 years, one may observe a long-term $\delta^{18}O$ trend containing the influence of atmospheric circulation change as well as the “amount effect".

Author contributions

T.-Y. Li and J. -Y. Li designed the research and revised the manuscript. H.-Y. Qiu and T. -Y. Li wrote the first version of the manuscript and revised it. C.-J. Chen, R. Huang, T. Wang, Y. Wu., S.-Y. Xiao, Y.-Z. Xu, Y.-Y. Huang and Yan Yang contributed to fieldwork and isotope measurements. All authors discussed the results and provided ideas to input the manuscript.

Declaration of competing interest

The authors declare that they have no known financial interests or personal relationships that could have appeared to influence the work reported in this paper.

Acknowledgements

This research was supported by the Open Project of Guangxi Key Science and Technology Innovation Base on Karst Dynamics (KDL &

Guangxi 202003) to J.-Y. Li, the National Natural Science Foundation of China (NSFC, No. 41772170; 42011530078), and the Fundamental Research Funds for the Central Universities, China (No. XDJK2017A010 and No. XDJK2020D005) to T.-Y. Li. We also give thanks to the editor and two anonymous reviewers for their constructive comments and suggestions.

References

Bar-Matthews, M., Ayalon, A., Matthews, A., Sass, E., Halicz, L., 1996. Carbon and oxygen isotope study of the active water-carbonate system in a karstic Mediterranean cave: implications for paleoclimate research in semiarid regions. Geochem. Cosmochim. Acta 60, 235–241.

Baker, A., Ito, E., Smart, P.L., Mcewan, R.F., 1997. Elevated and variable values of ^{13}C in speleothems in a British cave system. Chem. Geol. 136, 263–270.

Baker, A., Asrat, A., Fairchild, I.J., Leng, M.J., Wynn, P.M., Bryant, C., Genty, D., Umer, M., 2007. Analysis of the climate signal contained within $\delta^{18}O$ and growth rate parameters in two Ethiopian stalagmites. Geochem. Cosmochim. Acta 71, 2975–2988.

Baldini, J.U.L., McDermott, F., Hoffmann, D.L., Richards, D.A., Clipson, N., 2008. Very high-frequency and seasonal cave atmosphere pCO_2 variability: implications for stalagmite growth and oxygen isotope-based paleoclimate records. Earth Planet Sci. Lett. 272, 118–129.

Breitenbach, S.f.M., Lechleitner, F.A., Meyer, H., Diengdoh, G., Mattey, D., Marwan, N., 2015. Cave ventilation and rainfall signals in drip water in a monsoonal setting a monitoring study from NE India. Chem. Geol. 402, 111–124.

Coplen, T.B., Kendall, C., Hopple, J., 1983. Comparison of stable isotope reference samples. Nature 302, 236–238.

Chow, K.C., Tong, H.W., Chan, J.C.L., 2008. Water vapor sources associated with the early summer precipitation over China. Clim. Dynam. 30, 497–517.

Caballero, E., Cisneros, C.J.D., Reyes, E., 1996. A stable isotope study of cave seepage waters. Appl. Geochem. 11, 581–585.

Chen, C.-J., Li, T.-Y., 2018. Geochemical characteristics of cave drip water respond to ENSO based on a 6-year monitoring work in Yangkou Cave, Southwest China. J. Hydrol. 561, 896–907.

Comas-Bru, Laia, McDermott, Frank, 2015. Data-model comparison of soil-water delta O-18 at a temperate site in N. Spain with implications for interpreting speleothem delta O-18. J. Hydrol. 530, 216–224.

Coplen, T.B., 2007. Calibration of the calcite–water oxygen-isotope geothermometer at Devils Hole, Nevada, a natural laboratory. Geochem. Cosmochim. Acta 71, 3948–3957.

Cai, Z., Tian, L., 2016. Atmospheric controls on seasonal and interannual variations in the precipitation isotope in the East Asian Monsoon region. J. Clim. 29, 1339–1352.

Cai, Z.-Y., Tian, L.-D., Bowen, G.J., 2018. Spatial-seasonal patterns reveal large-scale atmospheric controls on Asian Monsoon precipitation water isotope ratios. Earth Planet Sci. Lett. 503, 158–169.

Cheng, H., Edwards, R.L., Wang, X.-F., Wang, Y.-J., Kong, X.-G., Yuan, D.-X., Zhang, M.-L., Lin, Y.-S., Qin, J.-M., Ran, J.-C., 2005. Oxygen isotope records of stalagmites from southern China. Quat. Sci. 25, 157–163 (in Chinese with English abstract).

Challa, V.S., Indrcanti, J., Baham, J.M., Patrick, C., Rabarison, M.K., Young, J.H., Hughes, R., Swanier, S.J., Hardy, M.G., Yerramilli, A., 2008. The sensitivity of atmospheric dispersion simulations by HYSPLIT to the meteorological predictions from a mesoscale model. Environ. Fluid Mech. 8, 367–387.

Cheng, H., Sinha, A., Wang, X., Cruz, F.W., Edwards, R.L., 2012. The global paleomonsoon as seen through speleothem records from asia and the americas. Clim. Dynam. 39, 1045–1062.

Cosford, J., Qing, H., Mattey, D., Eglington, B., Zhang, M., 2009. Climatic and local effects on stalagmite $\delta^{13}C$ values at Lianhua Cave, China. Paleogeogr. Palaeoclimatol. Palaeoecol. 280, 235–244.

Day, C.C., Henderson, G.M., 2011. Oxygen isotopes in calcite grown under cave-analogue conditions. Geochem. Cosmochim. Acta 75, 3956–3972.

Duan, W.-H., Ruan, J.-Y., Luo, W.-J., Li, T.-Y., Tian, L.-J., Zeng, G.-N., Zhang, D.-Z., Bai, Y.-J., Li, J.-L., Tao, T., Zhang, P., Baker, A., Tan, M., 2016. The transfer of seasonal isotopic variability between precipitation and drip water at eight caves in the monsoon regions of China. Geochem. Cosmochim. Acta 183, 250–266.

Dayem, K.E., Molnar, P., Battisti, D.S., Roe, G.H., 2010. Lessons learned from oxygen isotopes in modern precipitation applied to interpretation of speleothem records of paleoclimate from eastern Asia. Earth Planet Sci. Lett. 295, 219–230.

Dietzel, M., Tang, J., Leis, A., Köhler, S.J., 2009. Oxygen isotopic fractionation during inorganic calcite precipitation – Effects of temperature, precipitation rate and pH. Chem. Geol. 268, 107–115.

Dorale, J.A., Liu, Z., 2009. Limitations of hendy test criteria in judging the paleoclimatic suitability of speleothems and the need for replication. J. Cave Karst Stud. 71, 73–80.

Ding, Y.-H., Si, D., Sun, Y., Liu, Y.-J.L., Song, Y.-F., 2014. Inter-decadal variations, causes and future projection of the Asian summer monsoon. Eng. Sci. 2, 22–28.

Fairchild, I.J., Smith, C.L., Baker, A., Fuller, L., Spötl, C., Mattey, D., Mcdermott, F., E, I. M.F., 2006. Modification and preservation of environmental signals in speleothems. Earth Sci. Rev. 75, 105–153.

Feng, W., Casteel, R.C., Banner, J.L., Heinze-Fry, A., 2014. Oxygen isotope variations in rainfall, drip-water and speleothem calcite from a well-ventilated cave in Texas, USA: assessing a new speleothem temperature proxy. Geochem. Cosmochim. Acta 127, 233–250.

Fleitmann, D., Burns, S.J., Neff, U., Mudelsee, M., Mangini, A., Matter, A., 2004. Palaeoclimatic interpretation of high-resolution oxygen isotope profiles derived from annually laminated speleothems from Southern Oman. Quat. Sci. Rev. 23, 935–945.

Genty, D., Labuhn, I., Hoffmann, G., Danis, P.A., Mestre, O., Bourges, F., Wainer, K., Massault, M., Van Exter, S., Régnier, E., 2014. Rainfall and cave water isotopic relationships in two South-France sites. Geochem. Cosmochim. Acta 131, 323–343.

Hendy, C.H., 1971. The isotopic geochemistry of speleothems—I. The calculation of the effects of different modes of formation on the isotopic composition of speleothems and their applicability as palaeoclimatic indicators. Geochem. Cosmochim. Acta 35, 801–824.

Holmgren, K., Karlén, W.r., Shaw, P.A., 1995. Paleoclimatic significance of the stable isotopic composition and petrology of a late pleistocene stalagmite from Botswana. Quat. Res. 43, 320–328.

Hodge, E.J., Richards, D.A., Smart, P.L., Andreo, B., Hoffmann, D.L., Mattey, D.P., González-Ramón, A., 2008. Effective precipitation in southern Spain (~ 266 to 46? ka) based on a speleothem stable carbon isotope record. Quat. Res. 69, 447–457.

Hu, C.-Y., Henderson, G.M., Huang, J.-H., Xie, S., Sun, Y., Johnson, K.R., 2008. Quantification of Holocene Asian monsoon rainfall from spatially separated cave records. Earth Planet Sci. Lett. 266, 221–232.

Ishizaki, Y., Yoshimura, K., Kanae, S., Kimoto, M., Kurita, N., Oki, T., 2012. Interannual variability of $H_2^{18}O$ in precipitation over the Asian monsoon region. J. Geophys. Res. 117, D16308. https://doi.org/10.1029/2011JD015890.

Johnson, K.R., 2006. Seasonal trace-element and stable-isotope variations in a Chinese speleothem: the potential for high-resolution pale monsoon reconstruction. Earth Planet Sci. Lett. 244, 394–407.

Jin, Z.-H., Tao, S.-Y., 2002. The onset of the summer monsoon over the South China sea and its active and break periods. Climat. Environ. Res. 7 (3), 267–278. https://doi.org/10.3969/j.issn.1006-9585.2002.03.001 (in Chinese with English abstract).

Kim, S.T., O'Neil, J.R., Hillaire-Marcel, C., Mucci, A., 2007. Oxygen isotope fractionation between synthetic aragonite and water: influence of temperature and Mg^{2+} concentration. Geochem. Cosmochim. Acta 71, 4704–4715.

Kluge, T., Affek, H.P., Dublyansky, Y., Spötl, C., 2014. Devils Hole paleotemperatures and implications for oxygen isotope equilibrium fractionation. Earth Planet Sci. Lett. 400, 251–260.

Kuo, T.S., Liu, Z.Q., Li, H.C., Wan, N.J., Shen, C.C., Ku, T.L., 2011. Climate and environmental changes during the past millennium in central-western Guizhou, China as recorded by Stalagmite ZJD-21. J. Asian Earth Sci. 40, 1111–1120.

Linge, L., 2001. Stable isotope stratigraphy of Holocene speleothems: examples from a cave system in Rana, northern Norway. Palaeogeogr. Palaeoclimatol. Palaeoecol. 167, 209–224.

Liu, J.-R., Song, X.-F., Yuan, G.-F., Sun, X.-M., Liu, X., Wang, Z.-M., Wang, S.-Q., 2008. Stable isotopes of summer monsoonal precipitation in southern China and the moisture sources evidence from $\delta^{18}O$ signature. J. Geogr. Sci. 18, 155–165.

Laskar, A.H., Raghav, S., Yadava, M.G., Jani, R.A., Narayana, A.C., Ramesh, R., 2011. Potential of stable carbon and oxygen isotope variations of speleothems from andaman islands, India, for paleomonsoon reconstruction. J. Geol. Res. 2011, 1–7.

Lachniet, M.S., 2015. Are aragonite stalagmites reliable paleoclimate proxies? Tests for oxygen isotope time-series replication and equilibrium. Geol. Soc. Am. Bull. 127, 1521–1533.

Lee, J.E., Fung, I., Depaolo, D.J., Henning, C.C., 2007. Analysis of the global distribution of water isotopes using the NCAR atmospheric general circulation model. J. Geophys. Res. Atmos. 112, D16306. https://doi.org/10.1029/2006jd007657.

Li, H.-C., Lee, Z.H., Wan, N.-J., Shen, C.-C., Li, T.-Y., Yuan, D.-X., Chen, Y.H., 2011a. The $\delta^{18}O$ and $\delta^{13}C$ records in an aragonite stalagmite from Furong Cave, Chongqing, China: a-2000-year record of monsoonal climate. J. Asian Earth Sci. 40, 1121–1130.

Li, J.-Y., Li, H.-C., Li, T.-Y., Mii, H.-S., Yu, T.-L., Shen, C.-C., Xu, X., 2017. High-resolution $\delta^{18}O$ and $\delta^{13}C$ records of an A.M.S. 14-C and 230Th/U dated stalagmite from Xinya Cave in Chongqing: climate and vegetation change during the late Holocene. Quat. Int. 447, 75–88.

Li, J.-Y., Li, T.-Y., 2018. Seasonal and annual changes in soil/cave air pCO2 and the $\delta^{13}C$ DIC of cave drip water in response to changes in temperature and rainfall. Appl. Geochem. 93, 94–101.

Li, T.-Y., Shen, C.-C., Li, H.-C., Li, J.-Y., Chiang, H.-W., Song, S.-R., Yuan, D.-X., Lin, C.D. J., Gao, P., Zhou, L., Wang, J.-L., Ye, M.-Y., Tang, L.-L., Xie, S.-Y., 2011b. Oxygen and carbon isotopic systematics of aragonite speleothems and water in Furong Cave, Chongqing, China. Geochem. Cosmochim. Acta 75, 4140–4156.

Li, T.-Y., Li, H.-C., Xiang, X.-J., Kuo, T.S., Li, J.-Y., Zhou, F.-L., Chen, H.-L., Peng, L.-L., 2012. Transportation characteristics of $\delta^{13}C$ in the plants-soil-bedrock-cave system in Chongqing karst area. Sci. China Earth Sci. 55, 685–694.

Li, T.-Y., Huang, C.-X., Tian, L., Suarez, M., Gao, Y., 2018. Variation of $\delta^{13}C$ in plant-soil-cave systems in karst regions with different degrees of rocky desertification in southwest China. J. Cave Karst Stud. 80, 212–228.

Li, T.-Y., 2018. False amount effect—a discussion on one issue of isotope climatology. Quat. Sci. 38, 1545–1548 (in Chinese with English abstract).

Liu, D.-B., Wang, Y.-J., Cheng, H., Edwards, R.L., Kong, X.-G., Li, T.-Y., 2016. Strong coupling of centennial-scale changes of Asian monsoon and soil processes derived from stalagmite $\delta^{18}O$ and $\delta^{13}C$ records, southern China. Quat. Res. 85, 333–346.

Liu, J.-B., Chen, J.-H., Zhang, X.-J., Li, Y., Chen, F.-H., 2015. Holocene East Asian summer monsoon records in northern China and their inconsistency with Chinese stalagmite $\delta^{18}O$ records. Earth Sci. Rev. 148, 194–208.

Li, C.-Y., Qu, X., 2000. Large scale Atmospheric circulation evolutions associated with summer monsoon onset in the South China sea. Chin. J. Atmos. Sci. 24 (1), 1–14 (in Chinese with English abstract).

Moerman, J.W., Cobb, K.M., Partin, J.W., et al., 2014. Transformation of ENSO-related rainwater to drip water $\delta^{18}O$ variability by vadose water mixing. Geophys. Res. Lett. 41, 7907–7915.

Lü, J.-M., Zhang, Q.-Y., Tao, S.-Y., Ju, J.-H., 2006. The onset and advance of the Asian summer monsoon. Sci. Bull. 51 (1), 80–88 (in Chinese with English abstract).
McDonald, J., Drysdale, R., 2007. Hydrology of cave drip waters at varying bedrock depths from a karst system in southeastern Australia. Hydrol. Process. 21, 1737–1748.
Mickler, P.J., Stern, L.A., Banner, J.L., 2006. Large kinetic isotope effects in modern speleothems. Geol. Soc. Am. Bull. 118, 65–81.
Moore, M., Kuang, Z., Blossey, P.N., 2014. A moisture budget perspective of the amount effect. Geophys. Res. Lett. 41, 1329–1335.
Mickler, P.J., Banner, J.L., Stern, L., Asmerom, Y., Edwards, R.L., Ito, E., 2004. Stable isotope variations in modern tropical speleothems: evaluating equilibrium vs. kinetic isotope effects. Geochem. Cosmochim. Acta 68, 4381–4393.
Mühlinghaus, C., Scholz, D., Mangini, A., 2009. Modelling fractionation of stable isotopes in stalagmites. Geochem. Cosmochim. Acta 73, 7275–7289.
Nan, S., Tan, M., Zhao, P., 2014. Evaluation of the ability of the Chinese stalagmite $\delta^{18}O$ to record the variation in atmospheric circulation during the second half of the 20th century. Clim. Past 10 (3), 975–985.
Pape, J.R., Banner, J.L., Mack, L.E., Musgrove, M., Guilfoyle, A., 2010. Controls on oxygen isotope variability in precipitation and cave drip waters, central Texas, USA. J. Hydrol. 385, 203–215.
Perrin, J., Jeannin, P.Y., Zwahlen, F., 2003. Epikarst storage in a karst aquifer: a conceptual model based on isotopic data, Milandre test site, Switzerland. J. Hydrol. 279, 106–124.
Ruan, J., Zhang, H., Cai, Z., Yang, X., Yin, J., 2019. Regional controls on daily to interannual variations of precipitation isotope ratios in Southeast China: implications for paleomonsoon reconstruction. Earth Planet Sci. Lett. 527 https://doi.org/10.1016/j.epsl.2019.115794.
Riechelmann, D.F.C., Deininger, M., Scholz, D., Riechelmann, S., Schröder-Ritzrau, A., Spötl, C., Richter, D.K., Mangini, A., Immenhauser, A., 2013. Disequilibrium carbon and oxygen isotope fractionation in recent cave calcite: comparison of cave precipitates and model data. Geochem. Cosmochim. Acta 103, 232–244.
Sondag, F., Van, R.M., Soubies, F., Santos, R., Somerhausen, A., Seidel, A., Boggiani, P., 2003. Monitoring present day climatic conditions in tropical caves using an Environmental Data Acquisition System (EDAS). J. Hydrol. 273, 103–118.
Scholz, D., Frisia, S., Borsato, A., Spötl, C., Fohlmeister, J., Mudelsee, M., Miorandi, R., Mangini, A., 2012. Holocene climate variability in north-eastern Italy: potential influence of the NAO and solar activity recorded by speleothem data. Clim. Past 8, 1367–1383.
Stein, A.F., Draxler, R.R., Rolph, G.D., Stunder, B.J.B., Cohen, M.D., Ngan, F., 2015. NOAA's HYSPLIT atmospheric transport and dispersion modeling system. Bull. Am. Meteorol. Soc. 96, 2059–2077.
Sun, Z., Yang, Y., Zhao, J., Tian, N., Feng, X., 2018. Potential ENSO effects on the oxygen isotope composition of modern speleothems: observations from Jiguan Cave, central China. J. Hydrol. 566, 164–174.
Spötl, C., Fairchild, I.J., Tooth, A.F., 2005. Cave air control on dripwater geochemistry, Obir Caves (Austria): implications for speleothem deposition in dynamically ventilated caves. Geochem. Cosmochim. Acta 69, 2451–2468.
Treble, P.C., Chappell, J., Gagan, M.K., Mckeegan, K.D., Harrison, T.M., 2005. In situ measurement of seasonal $\delta^{18}O$ variations and analysis of isotopic trends in a modern speleothem from southwest Australia. Earth Planet Sci. Lett. 233, 17–32.
Tan, M., 2014. Circulation effect: response of precipitation $\delta^{18}O$ to the ENSO cycle in monsoon regions of China. Clim. Dynam. 42, 1067–1077.
Tan, M., 2016. Circulation background of climate patterns in the past millennium: uncertainty analysis and re-reconstruction of ENSO-like state. Sci. China Earth Sci. 59 (6), 1225–1241.
Tang, Y., Pang, H., Zhang, W., Li, Y., Wu, S., Hou, S., 2015. Effects of changes in moisture source and the upstream rainout on stable isotopes in precipitation – a case study in Nanjing, eastern China. Hydrol. Earth Syst. Sci. 19, 4293–4306.
Tremaine, D.M., Froelich, P.N., Wang, Y., 2011. Speleothem calcite farmed in situ: modern calibration of $\delta^{18}O$ and $\delta^{13}C$ paleoclimate proxies in a continuously-monitored natural cave system. Geochem. Cosmochim. Acta 75, 4929–4950.
Tan, M., 2009. Circulation effect: climatic significance of the short term variability of the oxygen isotopes in stalagmites from monsoonal China-dialogue between paleoclimate records and modern climate research. Quat. Sci. 29, 851–862 (in Chinese with English abstract).
Wackerbarth, A., Scholz, D., Fohlmeister, J., Mangini, A., 2010. Modelling the $\delta^{18}O$ value of cave drip water and speleothem calcite. Earth Planet Sci. Lett. 299, 387–397.
Wang, Y.-J., Cheng, H., Edwards, R.L., An, Z.S., Wu, J.-Y., Shen, C.-C., Dorale, J.A., 2001. A high-resolution absolute-dated late pleistocene monsoon record from hulu cave, China. Science 294, 2345–2348.
Wiedner, E., Scholz, D., Mangini, A., Polag, D., Mühlinghaus, C., Segl, M., 2008. Investigation of the stable isotope fractionation in speleothems with laboratory experiments. Quat. Int. 187, 15–24.
Wu, Y., Li, T.-Y., Yu, T.-L., Shen, C.-C., Chen, C.-J., Zhang, J., Li, J.-Y., Wang, T., Huang, R., Xiao, S.-Y., 2020. Variation of the Asian summer monsoon since the last glacial-interglacial recorded in a stalagmite from southwest China. Quat. Sci. Rev. https://doi.org/10.1016/j.quascirev.2020.106261.
Xie, L.-H., Wei, G.-J., Deng, W.-F., Zhao, X.-L., 2011. Daily $\delta^{18}O$ and δD of precipitations from 2007 to 2009 in Guangzhou, South China: implications for changes of moisture sources. J. Hydrol. 400, 477–489.
Yuan, D.-X., Cheng, H., Edwards, R.L., Dykoski, C.A., Kelly, M.J., Zhang, M.-L., Qing, J.-M., Lin, Y.-S., Wang, Y.-J., Wu, J.-Y., Dorale, J.A., An, Z.-S., Cai, Y.-J., 2004. Timing, duration, and transitions of the last interglacial Asian monsoon. Science 304, 575–578.
Yang, H., Johnson, K.R., Griffiths, M.L., Yoshimura, K., 2016. Interannual controls on oxygen isotope variability in Asian monsoon precipitation and implications for paleoclimate reconstructions. J. Geophys. Res. 121, 8410–8428.
Zeng, G.-N., Luo, W.-J., Wang, S.-J., Du, X.-L., 2015. Hydrogeochemical and climatic interpretations of isotopic signals from precipitation to drip waters in Liangfeng Cave, Guizhou Province, China. Environ. Earth Sci. 74, 1509–1519.
Zhang, H.-L., Yu, K.-F., Zhao, J.-X., Feng, Y.-X., Lin, Y.-S., Zhou, W., Liu, G.-H., 2013. East Asian Summer Monsoon variations in the past 12.5ka: high-resolution $\delta^{18}O$ record from a precisely dated aragonite stalagmite in central China. J. Asian Earth Sci. 73, 162–175.
Zhang, J., Li, T.-Y., 2019. Seasonal and interannual variations of hydrochemical characteristics and stable isotopic compositions of drip waters in Furong Cave, southwest China based on 12 years' monitoring. J. Hydrol. 572, 40–50.
Zhang, J., Genty, D., Sirieix, C., Michel, S., Minster, B., Régnier, E., 2020. Quantitative assessment of moisture source and temperature governing rainfall $\delta^{18}O$ from 20 years long monitoring records in SW-France: importance for isotopic-based climate reconstructions. J. Hydrol. 591, 1–20.
Zhou, J.-L., Li, T.-Y., 2018. A tentative study of the relationship between annual $\delta^{18}O$ and $\delta^{2}H$ variations of precipitation and atmospheric circulations—a case from Southwest China. Quat. Int. 479, 117–127.